Supplemental Material

Data S1.

Supplemental Methods

Drugs

Ibrutinib was obtained from Cellagen Technology (San Diego, CA) and acalabrutinb was obtained from ChemiTek (Indianapolis, IN). Trappsol (hydroxypropyl-β-cyclodextrin) was obtained from CT Holding Inc. (Alachua, FL).

In vivo electrophysiology

Mice were anesthetized with an intraperitoneal injection of ketamine (150 mg/kg) and xylazine (10 mg/kg) and placed in supine position on a heated water blanket. Body temperature was maintained at 36.5-37.5°C and monitored using a rectal probe.

A 2 french octapolar electrophysiology catheter (CIB'ER Mouse, NuMED) was inserted into the right jugular vein and advanced into the right atrium and right ventricle. Intracardiac electrograms were recorded at 1.5 kHz and filtered at 100-5000 Hz. All data were recorded using Acknowledge software (BIOPAC system). His bundle potential recordings were used to establish catheter positioning within the right atrium and right ventricle. Bipolar pacing was performed using 2 ms pulses at twice the diastolic threshold using a Grass SIU5 stimulus isolation unit and a Grass S99 stimulator. Refractory periods were measured using programmed electrical stimulation (PES) with a drive train of 9 stimuli (S1) at a cycle length of 100 ms followed by extra stimuli (S2) at progressively shorter cycle lengths. Atrial fibrillation susceptibility was measured using PES and burst pacing in the right atrium. AF was defined as a rapid and irregular atrial rhythm (fibrillatory baseline in the ECG) with irregular RR intervals lasting at least 1 s on the surface ECG.

High resolution optical mapping

To isolate atrial preparations, mice were administered a 0.2 ml intraperitoneal injection of heparin (1000 IU/ml) to prevent blood clotting and were then anesthetized by isoflurane inhalation and sacrificed by cervical dislocation. Hearts were excised into Krebs solution (37°C) containing (in mM): 118 NaCl, 4.7 KCl, 1.2 KH_2PO_4, 25 $NaHCO_3$, 1 $CaCl_2$, 1 $MgCl_2$, 11 glucose and bubbled with 95% O_2/5% CO_2 to maintain a pH of 7.4. The atria were dissected away from the ventricles and pinned in a dish with the endocardial surface facing upwards (towards the imaging equipment). The superior and inferior vena cavae were cut open so that the crista terminalis could be visualized, and the preparation could be pinned out flat with minimal tension.

The atrial preparation was superfused continuously with Krebs solution (37°C) bubbled with 95% O_2/5% CO_2 and allowed to equilibrate for ~10 min. The preparation was then incubated with the voltage sensitive dye RH-237 (15 µM; Biotium) for 5 min without superfusion. After the dye incubation period, superfusion was resumed with blebbistatin (10 µM; Cayman Chemical Company) added to the superfusate to suppress contractile activity and prevent motion artifacts. Experiments were performed in sinus rhythm so that the cycle length (i.e. beating rate) of the atrial preparation was free to change as well as in atrial preparations paced at a fixed cycle length of 125 ms (8Hz) in order to study electrical conduction independently of changes in beating rate. The pacing electrode was placed near the opening of the superior vena cava. RH-237-loaded atrial preparations were illuminated with light from a X-Cite Xylis Broad Spectrum LED Illumination System (Excelitas Technologies) and filtered with a 520/35 nm excitation filter (Semrock). Emitted fluorescence was separated by a dichroic mirror (560 nm cut-off; Semrock) and filtered by a 715 nm long-pass emissions filter (Andover Corp.). Recordings were captured using a high-speed CMOS camera (MiCAM03-N256, SciMedia). For mapping whole atrial preparations, data were captured from an optical field of view of 11 x 11 mm at a frame rate of 1000 frames/s using BrainVision software (BrainVision Inc.). The spatial resolution was 42.5 x 42.5 µM for each pixel. For mapping the right atrial posterior wall to

assess SAN function, data were captured from an optical field of view of 6.8 x 6.8 mm at a frame rate of 1000 frames/s. The spatial resolution was 26.6 x 26.6 μM for each pixel. Magnification was constant in all experiments and no pixel binning was used.

All optical data were analyzed using custom software written in MATLAB® (Mathworks). Pseudocolor electrical activation maps were generated from measurements of activation time at individual pixels as defined by assessment of dF/dt_{max} and background fluorescence was subtracted in all cases. Local conduction velocity (CV) was quantified specifically in the right atrial myocardium (within the right atrial appendage) and the left atrial myocardium (within the left atrial appendage) using established approaches previously described.[7,8] Briefly, activation times at each pixel from a 7 x 7 pixel array were determined and fit to a plane using the least squares fit method. The direction on this plane that is increasing the fastest represents the direction that is perpendicular to the wavefront of electrical propagation and the maximum slope represents the inverse of the speed of conduction in that direction. With a spatial resolution of 42.5 x 42.5 μM per pixel, the area of the 7 x 7 pixel array was 297.5 x 297.5 μM. This approach allows assessment the maximum local CV vectors in the atrial region of interest. Optical APs were assessed by measuring the change in fluorescence as a function of time at individual pixels within the right and left atria as we have done previously.

Atrial and sinoatrial node myocyte isolations

Mice were administered a 0.2 ml intraperitoneal injection of heparin (1000 IU/ml) to prevent blood clotting. Following this, mice were anesthetized by isoflurane inhalation and then sacrificed by cervical dislocation. The heart was excised into Tyrode's solution (35ºC) consisting of (in mM) 140 NaCl, 5.4 KCl, 1.2 KH_2PO_4, 1.0 $MgCl_2$, 1.8 $CaCl_2$, 5.55 glucose, and 5 HEPES, with pH adjusted to 7.4 with NaOH. Right and left atrial myocytes were isolated from the corresponding atrial appendages. The sinoatrial node (SAN) region of the heart was isolated by separating the atria from the ventricles, cutting open the superior and inferior venae cavae, and

pinning the tissue so that the crista terminalis could be identified. The SAN area is located in the intercaval region adjacent to the crista terminalis. Atrial and SAN tissue were cut into strips, which were transferred and rinsed in a 'low Ca^{2+}, Mg^{2+} free' solution containing (in mM) 140 NaCl, 5.4 KCl, 1.2 KH_2PO_4, 0.2 $CaCl_2$, 50 taurine, 18.5 glucose, 5 HEPES and 1 mg/ml bovine serum albumin (BSA), with pH adjusted to 6.9 with NaOH. Tissue strips were digested in 5 ml of 'low Ca^{2+}, Mg^{2+} free' solution containing collagenase (type II, Worthington Biochemical Corporation), elastase (Worthington Biochemical Corporation) and protease (type XIV, Sigma Chemical Company) for 30 min. Then the tissue was transferred to 5 ml of modified KB solution containing (in mM) 100 potassium glutamate, 10 potassium aspartate, 25 KCl, 10 KH_2PO_4, 2 $MgSO_4$, 20 taurine, 5 creatine, 0.5 EGTA, 20 glucose, 5 HEPES, and 0.1% BSA, with pH adjusted to 7.2 with KOH. The tissue was mechanically agitated using a wide-bore pipette. Atrial myocytes were quiescent and had stable resting membrane potentials when patch-clamped. SAN myocytes were identified by their small spindle shape and ability to beat spontaneously in the recording chamber when superfused with normal Tyrode's solution. When patch-clamped, SAN myocytes always displayed spontaneous action potentials.

Solutions and electrophysiological protocols

Spontaneous action potential (APs) in SAN myocytes and stimulated APs in atrial myocytes were recorded using the whole cell patch-clamp technique. Myocytes were superfused with normal Tyrode's solution (22 – 23ºC) containing (in mM): 140 NaCl, 5 KCl, 1 $MgCl_2$, 1 $CaCl_2$, 10 HEPES, and 5 glucose, with pH adjusted to 7.4 with NaOH. The pipette filling solution contained (in mM): 135 KCl, 0.1 $CaCl_2$, 1 $MgCl_2$, 5 NaCl, 10 EGTA, 4 Mg-ATP, 6.6 Na-phosphocreatine, 0.3 Na-GTP and 10 HEPES, with pH adjusted to 7.2 with KOH.

For recording I_{Na} atrial myocytes were superfused with a modified Tyrode's solution (22 – 23°C) containing the following (in mM): 130 CsCl, 5 NaCl, 5.4 TEA-Cl, 1 $MgCl_2$, 1 $CaCl_2$, 10 HEPES, 5.5 glucose, (pH 7.4, adjusted with CsOH). Nitrendipine (10 µM) was added to the

superfusate to block $I_{Ca,L}$. The pipette solution for I_{Na} contained (in mM): 120 CsCl, 5 NaCl, 1 $MgCl_2$, 0.2 $CaCl_2$, 10 HEPES, 5 MgATP, 0.3 Na-GTP, 5 BAPTA (pH 7.2, adjusted with CsOH). I_{Na} was recorded using 50 ms voltage clamp steps between -100 and +10 mV from a holding potential of -120 mV.

I_{Na} steady-state activation kinetics were determined by calculating chord conductance (G) with the equation $G=I/(V_m-E_{rev})$, where V_m represents the depolarizing voltages and E_{rev} is the reversal potential measured from the current-voltage relationships of $I_{Ca,L}$ or I_{Na}. Maximum conductance (G_{max}) and $V_{1/2}$ of activation ($V_{1/2(act)}$) for $I_{Ca,L}$ and I_{Na} were determined using the following function: $G=[(V_m-V_{rev})][G_{max}][-1/[(1+\exp((V_m-V_{1/2})/k))+1]]$. I_{Na} steady-state inactivation kinetics were measured using 500 ms pre-pulse voltage clamp steps between -120 and -30 mV from a holding potential of -120 mV followed by a 20 ms test pulse to -20 mV. Normalized peak currents were plotted as a function of the pre-pulse potential and the resulting curve was fitted with the Boltzmann function $h=1/[1+\exp[V_{1/2}-V]/k]$. These data were used to measure the voltage at which 50% of channels are inactivated ($V_{1/2(inact)}$).

For recording $I_{Ca,L}$ myocytes were superfused with a modified Tyrode's solution (22 – 23℃) containing the following (in mmol/L) 140 TEA-Cl, 5.4 CsCl, 2 $CaCl_2$, 1 $MgCl_2$, 10 HEPES, and 5 glucose with pH adjusted to 7.4 with CsOH. The pipette solution for $I_{Ca,L}$ contained (in mmol/L) 135 CsCl, 0.2 $CaCl_2$, 1 $MgCl_2$, 5 NaCl, 5 EGTA, 4 Mg-ATP, 6.6 Na-phosphocreatine, 0.3 Na-GTP and 10 HEPES, with pH adjusted to 7.2 with CsOH. $I_{Ca,L}$ was recorded using 250 ms voltage clamp steps between -60 mV and +40 mV from a holding potential of -60 mV in order to ensure measurement of $I_{Ca,L}$ generated by $Ca_V1.2$ and $Ca_V1.3$ channels. $I_{Ca,L}$ steady-state activation kinetics were quantified using the same formulas as for I_{Na} activation.

Total potassium currents (I_K) and I_f were recorded in the whole cell configuration of the patch clamp technique using the same Tyrode's solution and pipette solutions used to record APs. To record total potassium currents (no pre-pulse), cells were held at -80 mV then I_K was recorded using a series of voltage clamp steps (500 ms duration) between -120 and +80 mV in

10 mV increments. To record potassium currents with an inactivating pre-pulse (to inactivate I_{to}), cells were given a 200 ms pre-pulse to -40 mV immediately followed by 500 ms voltage clamp steps from -120 to +80 mV from a holding potential of -80 mV. For these recordings with and without a pre-pulse, I_K was measured at the peak current for each voltage step. I_{to} was calculated as the difference current between the recordings with and without a pre-pulse.

I_{Kur}, as carried by $K_V1.5$ channels, was measured as the component of I_K sensitive to 4-aminopyradine (4-AP; 100 µM). The voltage clamp protocol for measuring I_{Kur} included a pre-pulse to -40 mV for 200 ms to inactivate I_{to} immediately followed by a 500 ms step to +30 mV before returning to a holding potential of -80 mV. Peak currents at baseline, in the presence of 4-AP, and after washout were measured.

I_{Kr} was measured using a voltage clamp protocol designed to elicit outward $I_{K(tot)}$ and I_{Kr} tail currents. From a holding potential of -60 mV, cells were voltage clamped at potentials between -50mV and +40 mV for 1 s followed by a voltage clamp step to -45 mV for 2 s. I_{Kr} tail currents during the 2 s step to -45 mV were fit with the following Boltzmann function: $I=I_{max}/[1+\exp[-(V_m-V_{1/2})/k]]$.

I_f was recorded using 2 s voltage clamp steps between -30 and -140 mV followed by a voltage clamp step to -130 mV. The holding potential was -35 mV. $BaCl_2$ (1×10^{-4} mol/L) was added to the superfusate when recording I_f, in order to eliminate any inward rectifier K^+ current that could be present at low levels in some SAN myocytes. Activation kinetics for I_f were determined by normalizing tail currents at each voltage to the maximum current level at -130 mV and fitting the data to the Boltzmann function: $I/I_{max}=1/(1+\exp[(V_m-V_{1/2})/k])$ where V_m is the potential of the voltage clamp step, $V_{1/2}$ is the voltage at which 50% activation occurs and k is the slope factor.

Micropipettes were pulled from borosilicate glass (with filament, 1.5 mm OD, 0.75 mm ID, Sutter Instrument Company) using a Flaming/Brown pipette puller (model p-87, Sutter Instrument Company). The resistance of these pipettes was 4 – 8 MΩ when filled with recording

solution. Micropipettes were positioned with a micromanipulator (Burleigh PCS-5000 system) mounted on the stage of an inverted microscope (Olympus IX71). Seal resistance was 2 – 15 GΩ. Rupturing the sarcolemma in the patch experiments resulted in access resistances of 5 – 15 MΩ. Series resistance compensation averaged 80 – 85% using an Axopatch 200B amplifier (Molecular Devices). Data were digitized using a Digidata 1440 and pCLAMP 10 software (Molecular Devices) and stored on computer for analysis.

Table S1. Effects of ibrutinib on action potential parameters in right atrial myocytes.

	baseline	IBR(10)	washout
***n* (cells)**	10	10	9
Capacitance (pF)	41.0 ± 3.2	-	-
RMP (mV)	-81.4 ± 1.2	-80.6 ± 1.1	-82.5 ± 1.4
V_{max} (V/s)	147.3 ± 7.3	103 ± 11.9*	127.6 ± 11.1†
Overshoot (mV)	55.1 ± 2.2	37.5 ± 4.1*	51.8 ± 2.1†
APD_{20} (ms)	1.92 ± 0.3	2.72 ± 0.4*	1.98 ± 0.3†
APD_{50} (ms)	9.36 ± 0.9	18.7 ± 2.9*	10.4 ± 1.2†
APD_{70} (ms)	17.9 ± 1.5	41.5 ± 4.2*	19.3 ± 1.9†
APD_{90} (ms)	45.2 ± 2.4	77.4 ± 5.7*	41.4 ± 3.1†

IBR(10), 10μM ibrutinib; n, sample size; RMP, resting membrane potential; V_{max}, AP upstroke velocity; APD, action potential duration. APD values taken at 20, 50, 70, and 90% repolarization. Data are means ± SEM. *P<0.05 vs. baseline, †P<0.05 vs. IBR(10) by mixed-effects analysis with Tukey's post-hoc test.

Table S2. Effects of acalabrutinib on action potential parameters in right atrial myocytes.

	baseline	ACAL(10)	ACAL(50)	washout
***n* (cells)**	8	8	7	5
Capacitance (pF)	45.8 ± 5.5	-	-	-
RMP (mV)	-76.8 ± 0.5	-76.4 ± 0.8	-76.6 ± 0.8	-76.1 ± 1.4
V_{max} (V/s)	149.9 ± 7.9	148.2 ± 7.1	142.4 ± 7.6	146.5 ± 7.1
Overshoot (mV)	55.1 ± 3.3	56.6 ± 4.0	49.9 ± 4.3	54.8 ± 4.7
APD_{20} (ms)	2.37 ± 0.5	2.35 ± 0.5	2.38 ± 0.6	2.08 ± 0.8
APD_{50} (ms)	10.0 ± 1.5	12.2 ± 2.2	14.8 ± 2.6*	11.3 ± 3.7
APD_{70} (ms)	17.9 ± 2.3	21.0 ± 3.1	25.5 ± 3.2*	18.3 ± 4.6
APD_{90} (ms)	35.2 ± 3.0	38.4 ± 2.8	43.6 ± 4.7*	34.9 ± 5.0

ACAL(10), 10μM acalabrutinib; ACAL(50), 50μM acalabrutinib; n, sample size; RMP, resting membrane potential; V_{max}, AP upstroke velocity; APD, action potential duration. APD values taken at 20, 50, 70, and 90% repolarization. Data are means ± SEM. *P<0.05 vs. baseline by mixed-effects analysis with Tukey's post-hoc test.

Table S3. Effects of ibrutinib on action potential parameters in SAN myocytes.

	baseline	IBR(0.05)	washout
***n* (cells)**	11	11	7
Capacitance (pF)	33.8 ± 1.7	-	-
Cycle length (ms)	370.2 ± 7.9	452.6 ± 9.1*	381.7 ± 8.0
AP frequency (APs/min)	164.6 ± 2.2	133.1 ± 2.6*	157.6 ± 3.4
MDP (mV)	-66.6 ± 0.7	-65.2 ± 0.8*	-67.6 ± 0.7
DD Slope (mV/s)	40.4 ± 2.8	33.8 ± 2.8*	40.4 ± 2.3
V_{max} (V/s)	77.3 ± 6.4	68.3 ± 5.6*	70.5 ± 7.1
Overshoot (mV)	27.1 ± 2.9	22.1 ± 2.8*	18.6 ± 2.6*
APD_{50}	36.1 ± 3.6	51.9 ± 4.4*	37.9 ± 4.1

IBR(0.05), 0.05μM ibrutinib; n, sample size; MDP, maximum diastolic potential; DD slope, diastolic depolarization slope; Vmax, maximum AP upstroke velocity; APD_{50}, AP duration at 50% repolarization; Data are means ± SEM; **P*<0.05 vs baseline by mixed-effects analysis with Tukey's posthoc test.

Table S4. Effects of acalabrutinib on action potential parameters in SAN myocytes.

	baseline	ACAL(10)	washout
***n* (cells)**	5	5	5
Capacitance (pF)	38.9 ± 2.4	-	-
Cycle length (ms)	367.8 ± 11.6	363.8 ± 6.1	369.5 ± 10.6
AP frequency (APs/min)	163.7 ± 5.1	165.1 ± 2.8	162.9 ± 4.8
MDP (mV)	-65.3 ± 3.1	-68.4 ± 0.9	-67.7 ± 0.8
DD Slope (mV/s)	41.2 ± 5.1	42.7 ± 4.6	41.5 ± 3.8
V_{max} (V/s)	77.8 ± 7.6	73.7 ± 7.8	75.1 ± 10.6
Overshoot (mV)	30.0 ± 6.1	28.0 ± 5.8	30.7 ± 4.9
APD_{50}	47.2 ± 6.7	50.1 ± 7.6	39.4 ± 3.6

ACAL(10), 10μM acalabrutinib; n, sample size; MDP, maximum diastolic potential; DD slope, diastolic depolarization slope; Vmax, maximum AP upstroke velocity; APD_{50}, AP duration at 50% repolarization; Data are means ± SEM; **P*<0.05 vs baseline by two-way repeated measures ANOVA with Tukey's posthoc test.

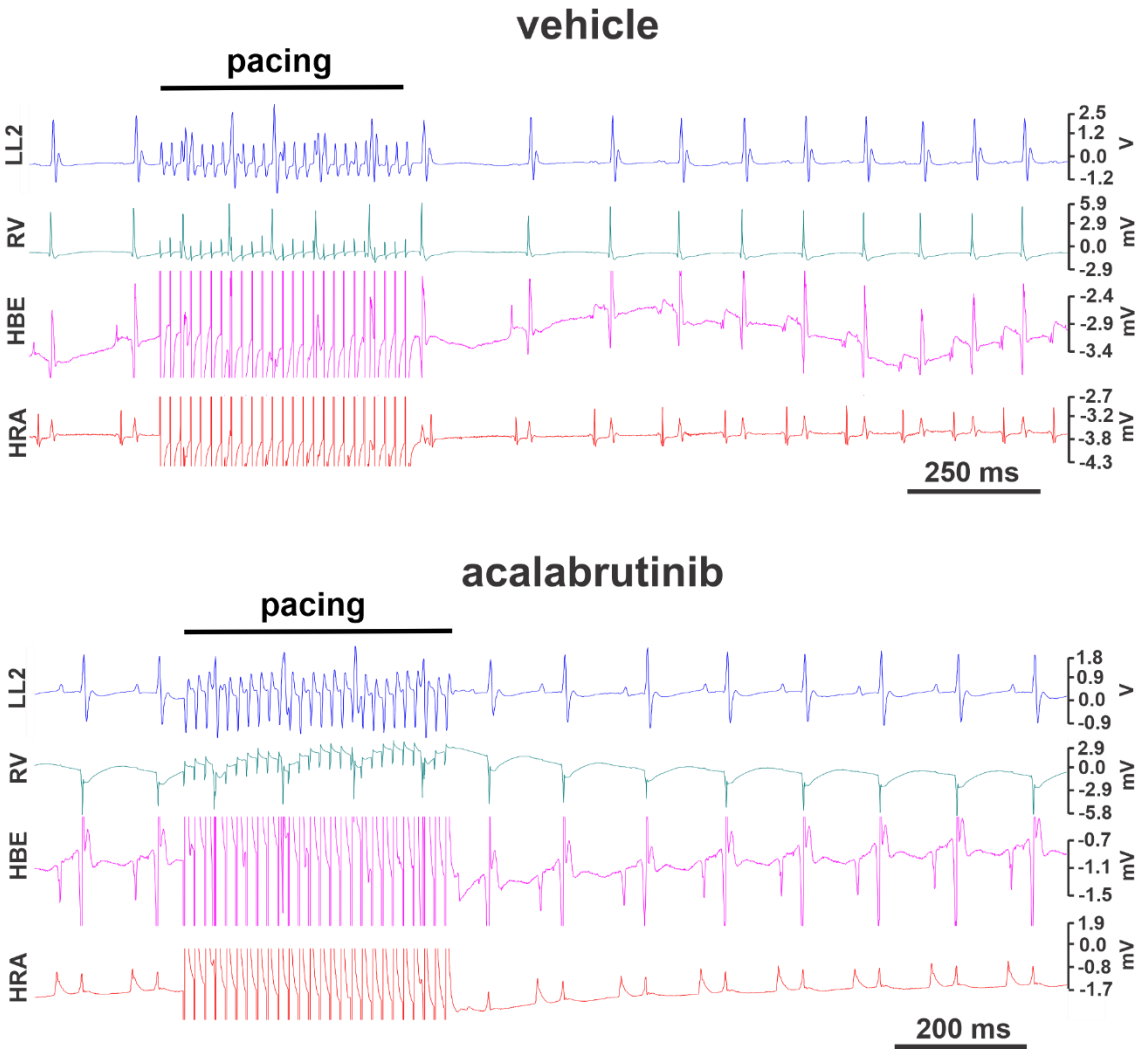

Figure S1. Absence of AF in mice treated with acalabrutinib. Representative surface electrocardiogram (ECG) and intracardiac recordings showing an absence of induction into AF after burst pacing in mice treated with acalabrutinib (10 mg/kg) or vehicle control. LL2, limb lead II; RV, right ventricle; HBE, His bundle region; HRA, high right atrium. Refer to Table 1 for summary data.

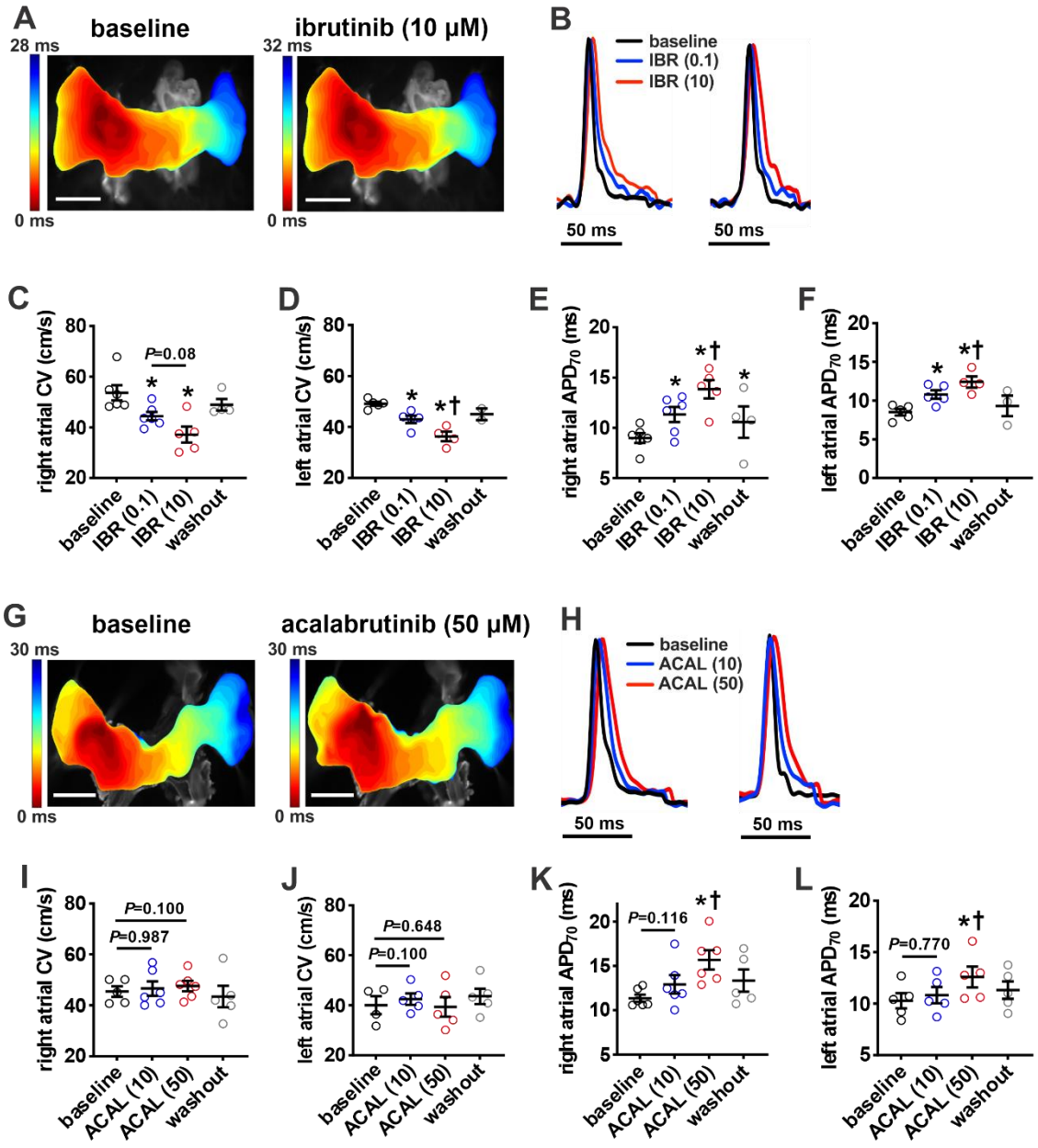

Figure S2. Effects of ibrutinib and acalabrutinib on atrial electrical conduction during pacing. A, Representative activation maps in isolated atrial preparations paced at 8 Hz at baseline and after superfusion with 10 μM ibrutinib. The right atrial appendage is on the left side of the image. Red indicates the earliest activation time. The colour scale indicates total conduction time across the atrial preparation. Scale bar: 2mm. **B,** Representative right (left) and left (right) atrial optical action potentials during pacing at 8 Hz at baseline and after superfusion with 0.1 μM ibrutinib (IBR(0.1)) or 10 μM ibrutinib (IBR(10)). **C** and **D,** Summary of local right (**C**) and left (**D**) atrial conduction velocities during pacing at 8 Hz. **E** and **F,** Summary of right (**E**) and left (**F**) atrial action potential duration at 70% repolarization (APD_{70}) during pacing at 8 Hz. For panels C-F *P<0.05 vs. baseline, †P<0.05 vs. IBR(0.1) by mixed effects analysis with a Tukey post-hoc test; n=4-6 atria per group. **G,** Representative activation maps from isolated atrial

preparations paced at 8 Hz at baseline and after superfusion with 50 μM acalabrutinib. Scale bar: 2mm. **H,** Representative right (left) and left (right) atrial optical action potentials during pacing at 8 Hz at baseline and after superfusion with 10 μM acalabrutinib (ACAL(10)) or 50 μM acalabrutinib (ACAL(50)). **I** and **J,** Summary of local right (**I**) and left (**J**) atrial conduction velocities during pacing at 8 Hz. **K** and **L,** Summary of right (**K**) and left (**L**) atrial APD_{70} during pacing at 8 Hz. For panels I-L $^{*}P<0.05$ vs. baseline, $^{\dagger}P<0.05$ vs. ACAL(10) by mixed effects analysis with a Tukey post-hoc test; n=4-6 atria per group.

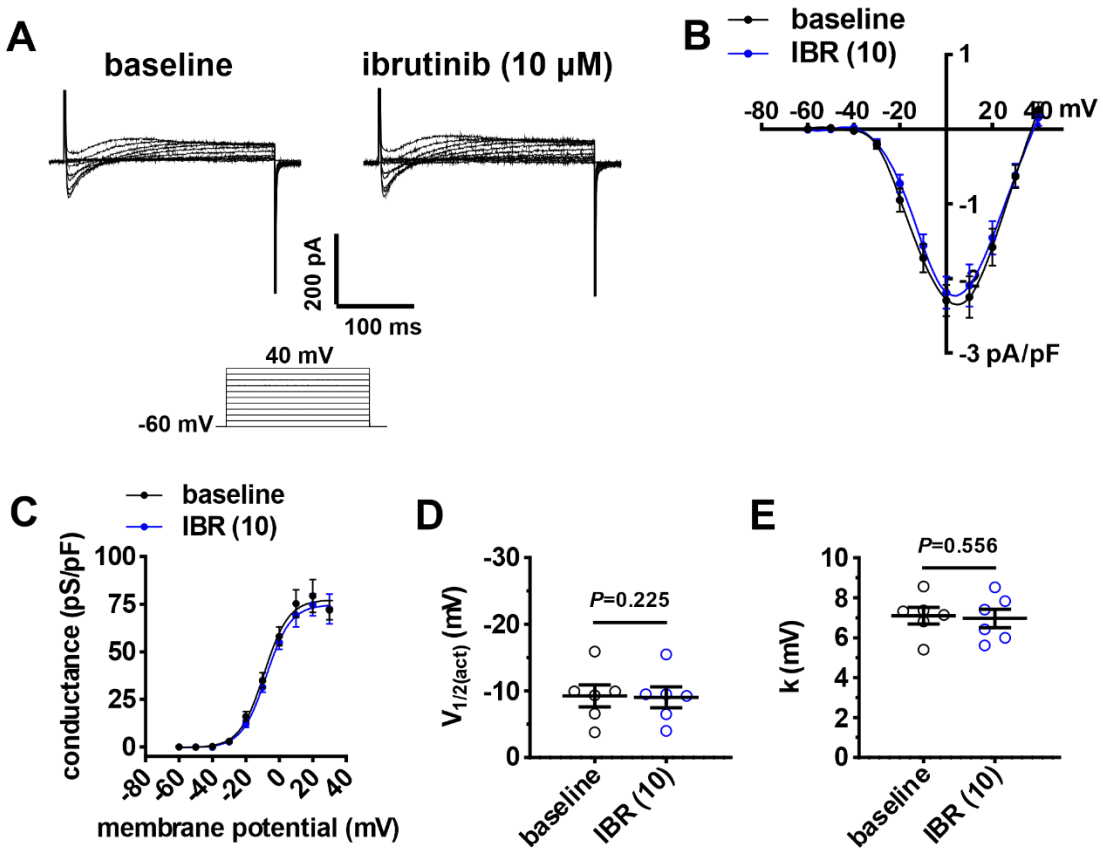

Figure S3. Effects of ibrutinib on $I_{Ca,L}$ in right atrial myocytes. A, Representative right atrial $I_{Ca,L}$ recordings as baseline and after application of 10 μM ibrutinib (IBR(10). Voltage clamp protocol shown below recordings. **B,** Right atrial $I_{Ca,L}$ IV curves at baseline and after application of IBR(10). **C,** Right atrial $I_{Ca,L}$ activation curves at baseline and after application of IBR(10). **D** and **E**, Summary of voltage for $I_{Ca,L}$ half maximum activation ($V_{1/2(act)}$; **D**) and $I_{Ca,L}$ slope factor (k, **E**) at baseline and after application of IBR(10). Data in panels B and C analyzed by mixed effects analysis with Tukey's post-hoc test, data in panels D and E analyzed by paired Student's *t*-test; *n*=6 right atrial myocytes from 3 mice.

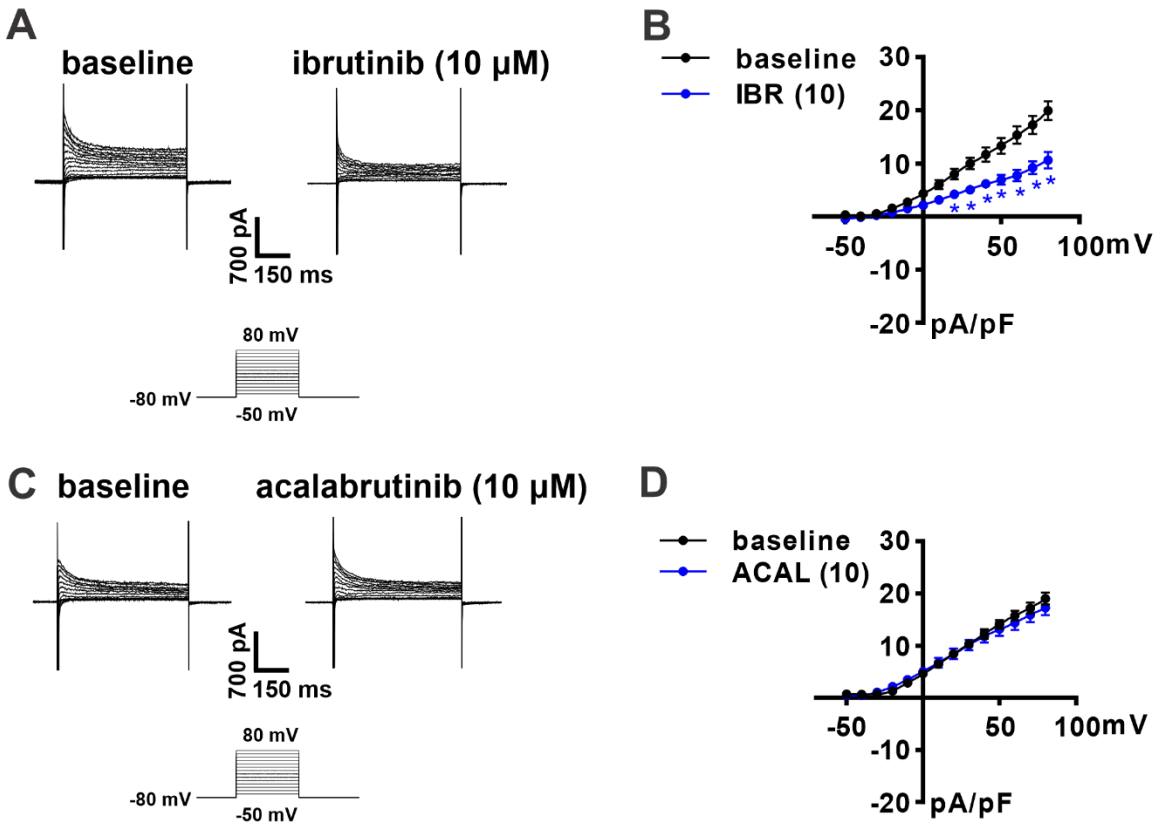

Figure S4. Effects of ibrutinib and acalabrutinib on repolarizing K^+ currents in isolated SAN myocytes. A, Representative SAN $I_{K(tot)}$ recordings at baseline and after application of 10 μM ibrutinib (IBR(10)). Voltage clamp protocol shown below recordings. **B,** Summary I_K IV curves measured at the peak of the $I_{K(tot)}$ recordings. **P*<0.05 vs. baseline by two-way repeated measures ANOVA with a Tukey posthoc test; *n*=7 SAN myocytes from 4 mice. **C,** Representative SAN $I_{K(tot)}$ recordings at baseline and after application of 10 μM acalabrutinib (ACAL(10)). Voltage clamp protocol shown below recordings. **D,** Summary I_K IV curves measured at the peak of the $I_{K(tot)}$ recordings. There was no difference between baseline and ACAL(10) by two-way repeated measures ANOVA with a Tukey posthoc test; *n*=6 SAN myocytes from 3 mice.

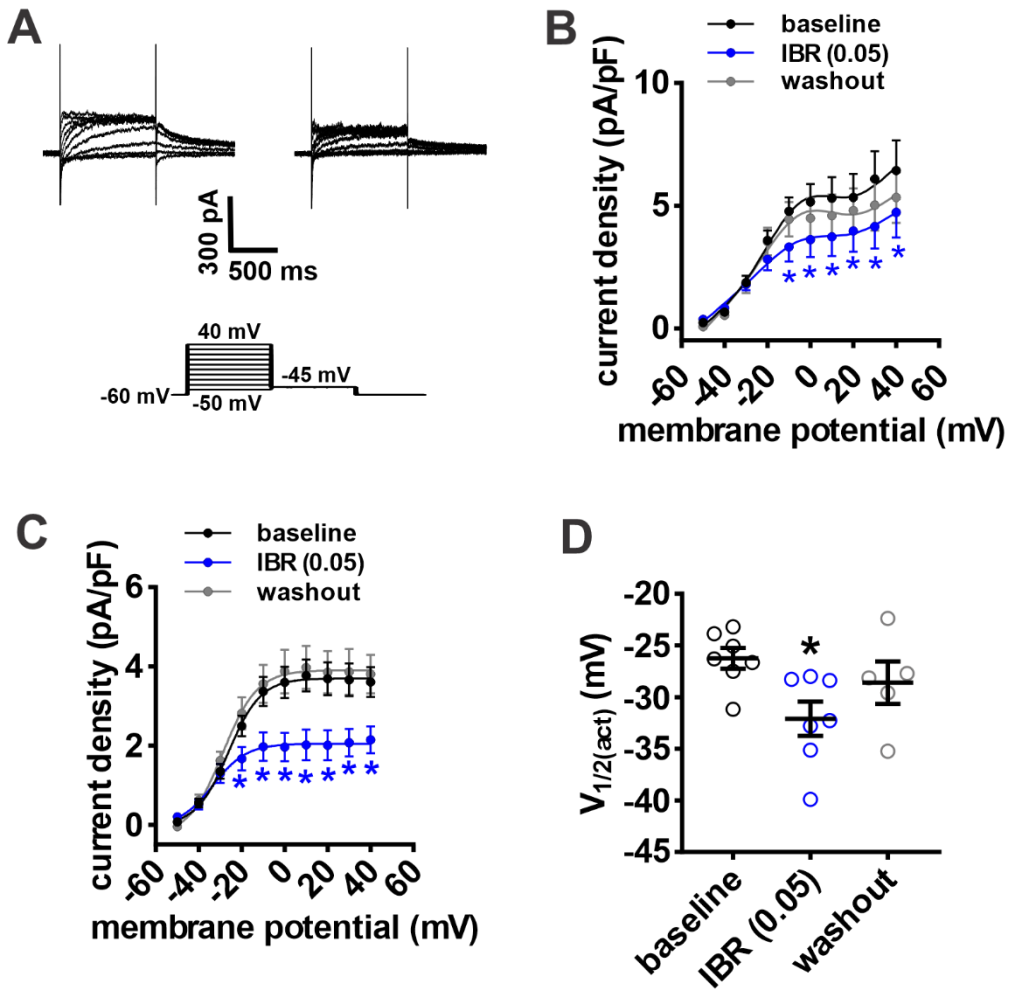

Figure S5. Effects of a lower dose of ibrutinib on the rapid delayed rectifier current (I_{Kr}) in isolated sinoatrial node (SAN) myocytes. A, Representative I_{Kr} recordings in isolated SAN myocytes at baseline and after application of 0.05 μM ibrutinib (IBR(0.05)). Voltage clamp protocol shown below recordings. **B,** Peak $I_{K(tot)}$ IV curves, measured at the end of the 1 s depolarizing steps, at baseline and after application of IBR(0.05). **C,** Boltzmann fit of I_{Kr} tail current at baseline and after application of IBR(0.05). **D,** Voltage for 50% channel activation ($V_{1/2(act)}$) for I_{Kr} tail current at baseline and after application of IBR(0.05). For panels B-C **P*<0.05 vs. baseline by mixed effects analysis with a Tukey post-hoc test; for panel D **P*<0.05 vs. baseline by mixed effects analysis with Tukey's post-hoc test; *n*=7 SAN myocytes from 3 mice.

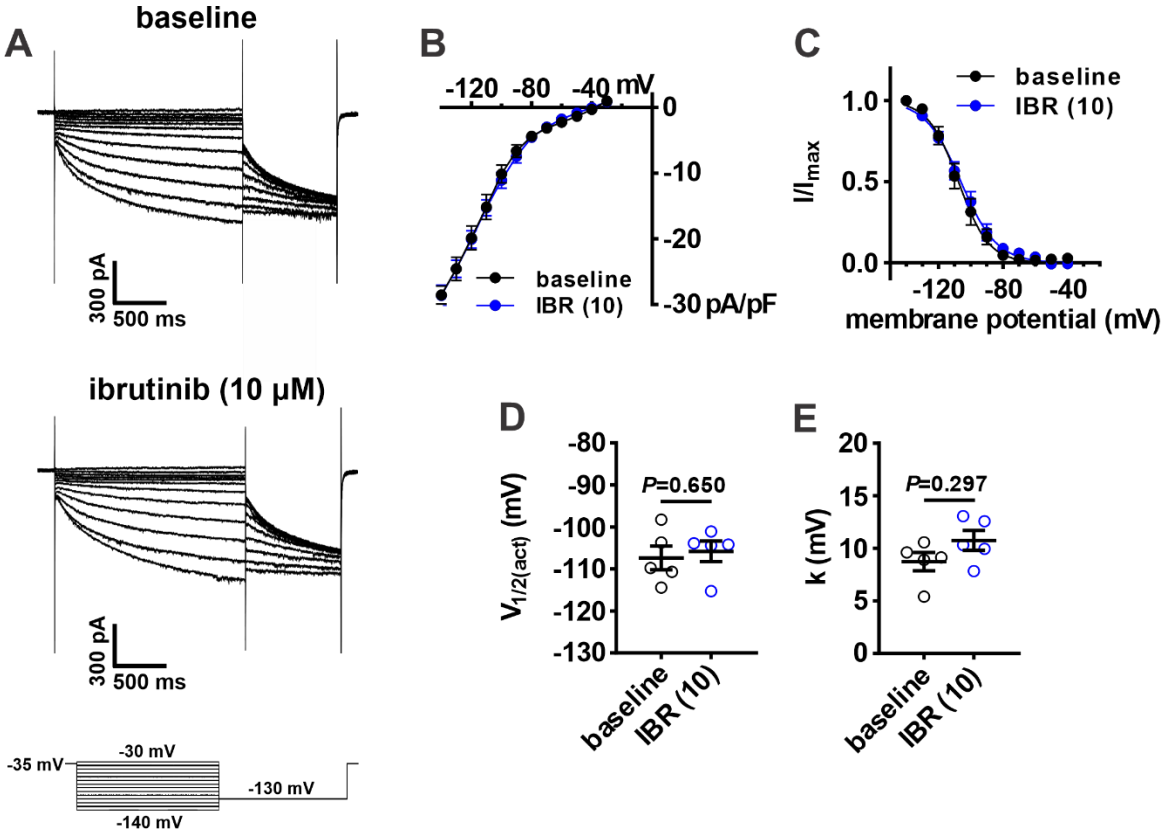

Figure S6. Effects of ibrutinib on the hyperpolarization activated current (I_f) in SAN myocytes. A, Representative I_f recordings at baseline and after application of 10 µM ibrutinib (IBR(10)). **B,** I_f IV curves at baseline and after application of IBR(10). I_f activation curves at baseline and after application of IBR(10)). **D** and **E**, effects of IBR(10) on I_f $V_{1/2(act)}$ (**D**) and slope factor (k, **E**). IBR(10) had no effects of I_f amplitude or activation kinetics. Data in panels B and C analyzed by two-way repeated measures ANOVA with a Tukey posthoc test; data in panels D and E analyzed by paired Student's *t*-test; *n*=5 SAN myocytes from 3 mice.

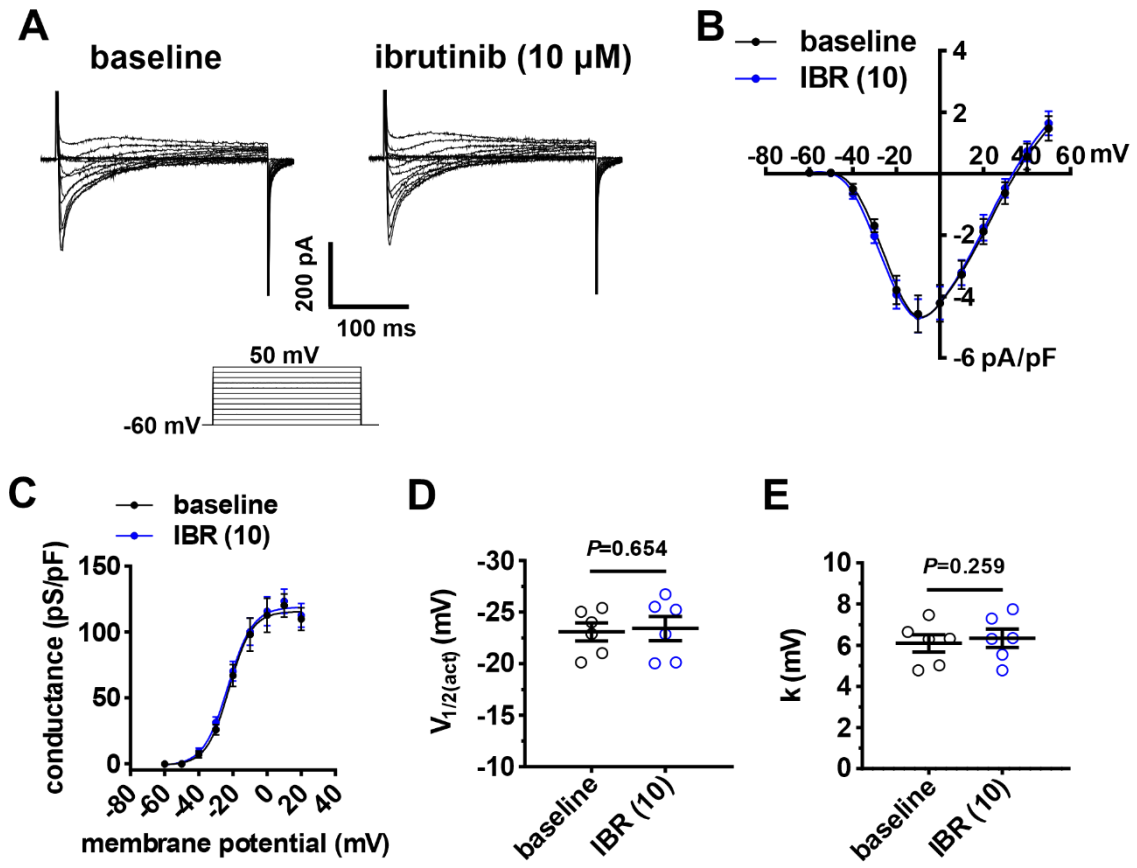

Figure S7. Effects of ibrutinib on $I_{Ca,L}$ in sinoatrial node myocytes. A, Representative SAN $I_{Ca,L}$ recordings as baseline and after application of 10 μM ibrutinib (IBR(10). Voltage clamp protocol shown below recordings. **B,** SAN $I_{Ca,L}$ IV curves at baseline and after application of IBR(10). **C,** SAN $I_{Ca,L}$ activation curves at baseline and after application of IBR(10). **D** and **E**, Summary of voltage for $I_{Ca,L}$ half maximum activation ($V_{1/2(act)}$; **D**) and $I_{Ca,L}$ slope factor (k, **E**) at baseline and after application of IBR(10). Data in panels B and C analyzed by mixed effects analysis with Tukey's post-hoc test, data in panels D and E analyzed by paired Student's *t*-test; *n*=6 SAN myocytes from 3 mice.